Title: Metabolic Endotoxemia Induces Sex-Specific Temporomandibular Joint Osteoarthritis via Leptin Signalling in Rats

Authors:

1. Shipin Zhang, B.D.S, Ph.D.[1*] (https://orcid.org/0000-0001-8421-7108)

2. Siyi Chen, M.Sc.[1] (https://orcid.org/0009-0008-6462-4441)

3. Marina Fonti, Ph.D.[1] (https://orcid.org/0000-0002-2415-8019)

4. David Fercher, M.Sc.[1] (https://orcid.org/0009-0000-8934-9441)

[*] Corresponding author: shipin.zhang@hest.ethz.ch

Authors' affiliation: [1]Department of Health Sciences and Technology, Institute for Biomechanics, Tissue Engineering and Biofabrication Group, ETH Zürich, Switzerland

Keywords: Metabolic Endotoxemia, Temporomandibular joint, Osteoarthritis, Leptin Signalling, Sex Difference, Adipose Tissue Dysfunction

Abstract

Objective: Temporomandibular joint (TMJ) osteoarthritis (OA) is a degenerative disease affecting the whole synovial joint, with a higher prevalence in women. While obesity is recognised as a risk factor for knee OA, its association with TMJ degeneration remains controversial. Recently, metabolic endotoxemia, characterised by a subclinical elevation of circulating lipopolysaccharide (LPS), has been proposed as a key mediator of obesity. It was thought to accelerate OA progression in knee joints by triggering low-grade systemic inflammation. However, the contribution of endotoxemia to TMJ OA is unclear. This study investigated whether chronic LPS exposure induces TMJ OA and whether its interplay with adipose tissue is involved in this process, particularly in a sex-specific context.

Methods: Metabolic endotoxemia was induced in 6-month-old female and male Wistar rats by continuous subcutaneous infusion of LPS for 4 - 6 weeks using osmotic pumps. Ten weeks after the start of LPS infusion, peripheral blood, subcutaneous and visceral white adipose tissue, and TMJs were harvested for biochemical, histological, micro-computed tomography and gene expression analyses. Primary TMJ chondrocytes isolated from healthy female and male rats were further used to assess sex-specific responses to leptin and LPS in vitro.

Results: Chronic LPS exposure induced pronounced OA-like changes in female TMJs, including cartilage matrix loss, subchondral bone resorption and mild synovial inflammation, whereas male joints were minimally affected. In female cartilage, immunofluorescence analyses showed an increased proportion of cells co-expressing leptin, leptin receptor and inducible nitric oxide synthase, supporting local activation of leptin-associated inflammatory pathways. In contrast, LPS immunosignal was not detected in cartilage. Systemically, LPS-treated female rats exhibited elevated circulating LPS and leptin concentrations, together with adipocyte hypertrophy and inflammatory changes in subcutaneous adipose tissue, whereas these changes were not evident in males. *In vitro*, leptin induced stronger metabolic and inflammatory responses in female chondrocytes, including reduced intracellular lipid content and metabolic activity, increased nitric oxide production, and upregulated catabolic gene expressions following LPS priming.

Conclusion: Chronic systemic LPS exposure induced sex-specific TMJ OA associated with adipose tissue dysfunction and altered leptin signalling. These findings support a potential female-biased systemic-to-local adipose-cartilage link between endotoxemia and TMJ OA pathogenesis.

1. Introduction

The temporomandibular joint (TMJ) is a synovial joint in the craniofacial region that experiences mechanical loading when functioning [1, 2]. TMJ osteoarthritis (OA) is a degenerative disease featured by cartilage surface fibrillation, glycosaminoglycan (GAG) loss, bone remodelling and synovitis, and is significantly more prevalent in females than males [3-5].

Recently, metabolic osteoarthritis (MetOA) has been recognized as a subtype of OA that is associated with systemic low-grade inflammation, oxidative stress, adipose dysregulation, and other metabolic changes [6-8], often linked to high body mass index (BMI) and obesity [9, 10]. While the association between obesity and knee OA is well established, the relationship between body mass and TMJ OA remains controversial. Population studies have suggested that high BMI is not a risk factor for TMJ disorders (TMD) and may even be a protective factor for TMD pain [11, 12], whereas preclinical results have shown that high-fat-diet (HFD)-induced obesity promotes TMJ OA [13, 14]. The discrepancy between human and animal studies suggests high body mass alone may not fully explain the relationship between obesity and TMJ OA. This raises the possibility that specific obesity-associated systemic factors, rather than increased body mass per se, drive the development of TMJ OA.

Metabolic endotoxemia, defined as a subclinical elevation of circulating endotoxin (lipopolysaccharide, LPS) [15], has emerged as a potential key mediator. Elevated LPS levels have been observed in obese individuals [16, 17] and diet-induced obese rodents [15, 18, 19]. LPS has been implicated in the pathogenesis of knee arthritis [15, 20-22] by inducing systemic inflammation and modulating immune responses [23]. However, whether metabolic endotoxemia contributes to TMJ OA and how it interacts with adipose tissue in this context remains unclear. Furthermore, the mechanisms underlying sex differences in OA development are not fully understood.

To address these gaps, we investigated the effects of chronic systemic LPS exposure on TMJ OA development in male and female rats, with particular focus on the involvement of adipose tissue and leptin, an OA-related adipokine [24]. We administered LPS systemically for 6 weeks and subsequently assessed osteoarthritic changes in the TMJ, systemic inflammatory markers, adipose tissue alterations, and adipokine profiles. Additionally, we evaluated sex-dependent effects of LPS and leptin on female and male TMJ condylar chondrocytes *in vitro*.

2. Method:

The primer list and detailed study protocols were included in the Supplementary Method.

2.1 Animal experiment

The animal study was approved by the Veterinary Office of the Canton Zürich (License No. ZH158/2021) and conducted in accordance with ARRIVE guidelines. Thirteen male and fourteen female Wistar rats (6 months old, Janvier Labs, France) with a mean weight of male:485 g (372 – 632 g) and female: 291 g (253 – 330 g) were used. A pilot trial involving 6 females and 5 males was conducted to determine the animals' tolerance to chronic LPS infusion and to calculate the required sample size to achieve 80% study power. In this trial, animals were randomly allocated into the LPS group (2 males and 3 females) and the saline

control group (3 males and 3 females). Rats were implanted subcutaneously with osmotic pumps (Alzet 2ML4, DURECT Corporate, USA), as previously described [25]. The pump was either filled with 0.9% Sodium chloride (NaCl) (B.Braun, Germany) or LPS from Escherichia coli (*E. coli*) O26:B6 (Sigma-Aldrich, USA) to infuse 18 µg/kg/day LPS for 4 weeks (Figure 1A). In the main trial, the animals were randomised into Control or LPS group (n = 4 per sex and group) by block randomization method [26]. Osmotic pumps (Alzet 2006) were used to continuously deliver either 0.9% NaCl or LPS at 18 µg/kg/day for 6 weeks (Figure 1B). In both trials, animals were housed in groups of 2 or 3 in individually ventilated cages in a standard laboratory animal environment (21± 3 °C and 12/12h light–dark cycle), received acidified tap water (pH 2.5-3.0) and standard laboratory rodent diet (KLIBA NAFAG, CH) in a specific opportunistic pathogen-free facility. After ten weeks, animals were euthanized by CO_2 overdose. Whole blood, TMJ condyles, rat heads, dorsolumbar subcutaneous adipose tissue (SAT) and the mesenteric visceral adipose tissue (VAT) were collected [27], for various analyses.

Primary TMJ condylar chondrocytes were isolated from 8-month-old healthy rat carcasses (2 males and 2 females) obtained as surplus material from another study (Figure 1C).

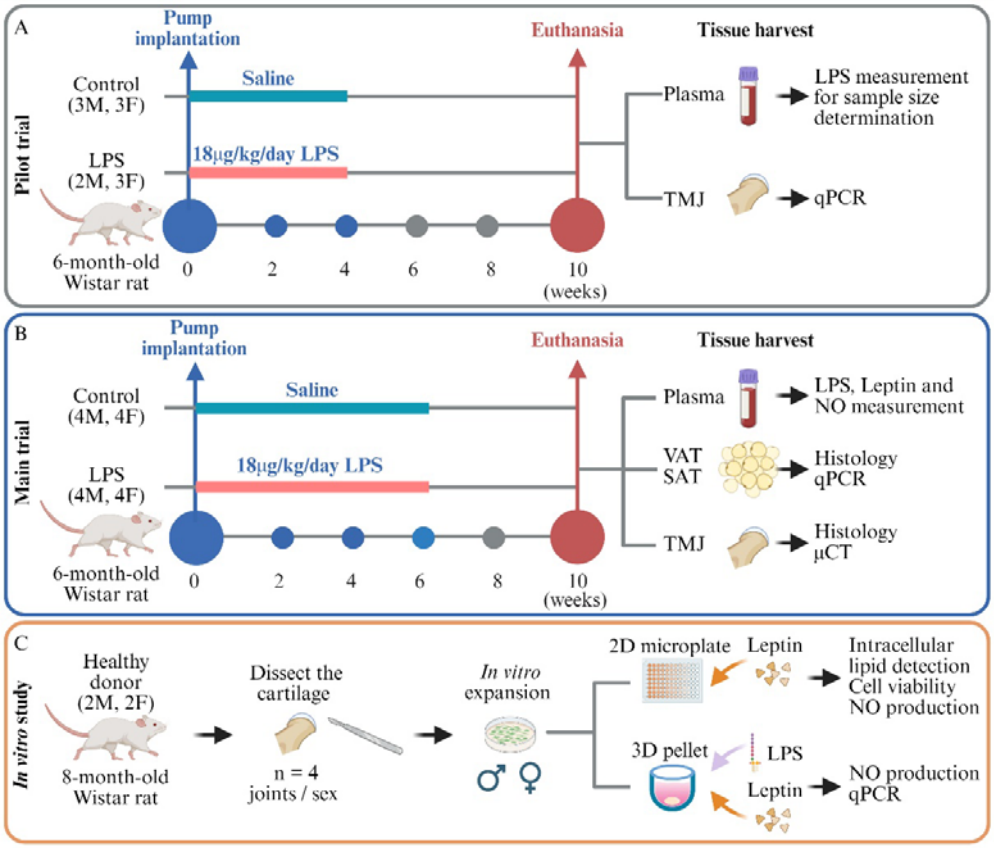

Figure 1. Schematic illustration of *in vivo* and *in vitro* experiment design. Schematic of animal groups, study timeline and tissue harvest plans for (A) pilot trial and (B) main trial. (C) *In vitro* experimental setup to study the role of leptin in OA development. M: Male; F: Female. In the pilot trial, blood was collected to measure LPS concentration, and TMJ condyles were harvested for qPCR-based gene expression analysis. In the main trial, blood was collected to

measure LPS, nitric oxide (NO), and leptin. Subcutaneous adipose tissue (SAT) and visceral adipose tissue (VAT) were collected for qPCR-based gene expression analysis and histomorphometry evaluation. The heads were collected for micro-computed tomography bone analysis and histology evaluation. For the *in vitro* study, TMJ condylar chondrocytes were isolated from healthy rat joints and used for mechanistic evaluations. Created in BioRender. Zhang, S. (2026) https://BioRender.com/vdjaeod

2.2 Blood analysis

5 mL whole blood was collected post-mortem via cardiac puncture into a BD Vacutainer® EDTA Tubes (BD, USA), centrifuged for 10 min at 1500 g to remove cells, then for 10 min at 2000 g to deplete platelets from plasma. Plasma was diluted 50-fold with endotoxin-free water for LPS concentration analysis by the LAL assay kit (Thermofisher), 30-fold for nitric oxide (NO) quantification using Griess reagent kit (Thermofisher), or 3-fold for leptin quantification using an ELISA kit (Merck). Assays were performed according to manufacturers' instructions.

2.3 Micro-computed tomography evaluation

The heads were dissected and fixed at 4% (v/v) paraformaldehyde (PFA). High-resolution micro-computed tomography (µCT) (µCT45, SCANCO MEDICAL) was performed to assess bone morphology. For bone parameter analysis, a stack of 200 coronal slides across the entire condyle were selected. The percentage of bone volume over total volume (BV/TV, %), trabecular thickness (Tb.Th, µm), trabecular separation (Tb.Sp, µm), trabecular number (Tb.N, 1/mm), and bone mineral density (BMD) were quantified using CTAn version 1.13 (Bruker microCT, Kontich, Belgium).

2.4 Histomorphometric analysis

SAT, VAT and TMJs were paraffin-embedded [28], cut at 5 µm, and stained with haematoxylin and eosin (HE) for general morphology. TMJs were stained for Safranin-O/fast green (Saf-O) for GAG deposition, picrosirius red (PSR) for fiber orientation [29], and immunohistochemistry (IHC) to detect the distribution of type II collagen (Col II) [30] or inducible nitric oxide (iNOS) in condylar cartilage [31]. Immunofluorescent (IF) staining was performed to detect the expression and colocalization of iNOS, leptin and leptin receptor (OB-R) in chondrocytes. Mankin scoring [32] was performed on Saf-O-stained TMJs to evaluate cartilage degeneration. Krenn's synovitis score [33] was performed on HE-stained slides to assess the synovial inflammation. Both scorings were performed independently by two blinded observers (S.Z and M.F). QuPath v0 and ImageJ software (National Institutes of Health) were used for semi-quantitative image analysis of adipocyte size, Saf-O- and Col II-stained area, percentage of iNOS-positive ($iNOS^+$), Leptin-positive cells ($Leptin^+$), OB-R-positive cells ($OB\text{-}R^+$), and iNOS/Leptin/OB-R triple-positive ($Triple^+$) cells over total cells. The collagen fiber orientation in condylar cartilage was measured using OrientationJ [34].

2.5 In vitro mechanistic study

TMJ condylar chondrocytes were isolated and cultured using a method adapted from Zhang et al [31]. For the 2D microplate assay, 5000 chondrocytes were seeded per well in a 96-well plate overnight to allow cell adhesion, then stimulated with 1, 2, 5, 10, or 20 ng/ml of rat leptin

(PeproTech) for 24 hours. At the end of the treatment, MTS assay (Abcam) was performed to measure the cellular metabolism. Cell culture supernatant was collected for NO quantification. Nile red staining was performed on the cells to visualise intracellular lipid droplets. For the 3D pellet assay, the chondrocyte pellets were prepared [31], and stimulated with 100 ng/ml LPS for 24 hours, followed by 20 ng/ml leptin for 24 hours. The culture supernatant was collected for NO quantification. The chondrocyte pellets were lysed for Picogreen DNA quantification (Thermofisher) per the manufacturer's instructions and for gene expression analysis (Figure 1C).

2.6 RNA isolation and qRT-PCR analysis

RNA extraction from chondrocyte pellets was performed with the RNeasy® kit (Qiagen) according to the manufacturer's instructions. RNA extraction from adipose tissue and TMJ condyles was performed as previously described [29]. Gene expression heatmap of TMJ condyles was generated using Morpheus (https://software.broadinstitute.org/morpheus/). Samples were hierarchically clustered using one minus Pearson correlation as the metric and average linkage as the linkage method, and stratified by sex. Genomic DNA was extracted from chondrocytes to verify the biological sex of cells using a single-step PCR-based method [35].

2.7 Statistics

Blood LPS concentration from the pilot trial was used to calculate the sample size using G*Power 3.1.3 [36, 37]. Number (n) = 3 animals per group per sex was estimated to provide 80% power with a significance level of $p = 0.05$ (two-tailed) to detect differences between treatments in females and between sexes in the LPS group. Each animal is counted as one experimental unit for blood analysis, adipose size quantification, and weight change. Left and right joints from the same animal were averaged and treated as a single biological replicate for semi-quantification of Saf-O$^+$ area, Col II$^+$ area, % iNOS$^+$ in the whole cartilage, histological scorings, fiber orientation analysis, µCT evaluation and IF quantification. Unless otherwise stated, all data were presented as mean (95% CI) and were compared by either two-way (Treatment x Sex) or three-way (treatment x sex x time; or treatment x sex x fat) ANOVA with Fisher's LSD or Sidak *post hoc* tests where appropriate. Mann-Whitney U tests were used to compare two groups for datasets that failed normality tests (Q-Q plot and Shapiro-Wilk). The interclass correlation coefficient (ICC) was calculated to assess the agreement between the two independent observers' histopathological scores. The statistical significance level was set at $P < 0.05$. SPSS version 29.0 (IBM, Chicago, IL, USA) was used for Mann-Whitney U, ICC. Other analyses were performed in GraphPad Prism 10 (GraphPad Software, LLC).

3. Results

3.1 LPS induced more severe TMJ osteoarthritic changes in females

LPS-infused male animals showed slight surface fibrillation, loss of cells and matrix in the superficial layer (Figure 2A and Supplementary Figure 1). In comparison, LPS-infused females exhibited greater loss of GAG and Col II throughout the whole cartilage layer (Figure 2A and Supplementary Figure 2). Consistently, the total Mankin score was marginally higher

in LPS-treated animals than in controls (Figure 1B), with LPS-treated males showing more destructive changes in surface regularity and cellularity, and LPS-treated females exhibiting greater extracellular matrix (ECM) loss (Supplementary Figures 1-2). This was further confirmed by semi-quantitative analysis of GAG and collagen II deposition. Relative to same sex controls, LPS-treated female rats had 15% less Saf-O$^+$ area (35.42%, 95%CI: 26.20 – 44.64% *vs.*50.76%, 95%CI: 35.78 – 65.74%, P = 0.02), and 9% less Col II$^+$ area (58.41%, 95%CI: 51.46 – 65.36% *vs.*67.04%, 95%CI: 57.22 – 76.86%, P = 0.05) in the whole cartilage, whereas LPS-treated males exhibited no reduction in the Saf-O$^+$ area, and only 5% loss of Col II$^+$ (Figure 2C, D). Collagen fibre derangement was visualised in pseudo-colour maps based on polarized PSR images (Figure 2A and Supplementary Figure 3). Fibres in the superficial zone were oriented more parallel to the cartilage surface in LPS-treated females (6.84°, 95%CI: 5.45 – 8.23° vs 11.81°, 95%CI: 4.26 – 19.36°) compared to controls. The change in fibre orientation is pronounced in LPS-treated males (Figure 2E).

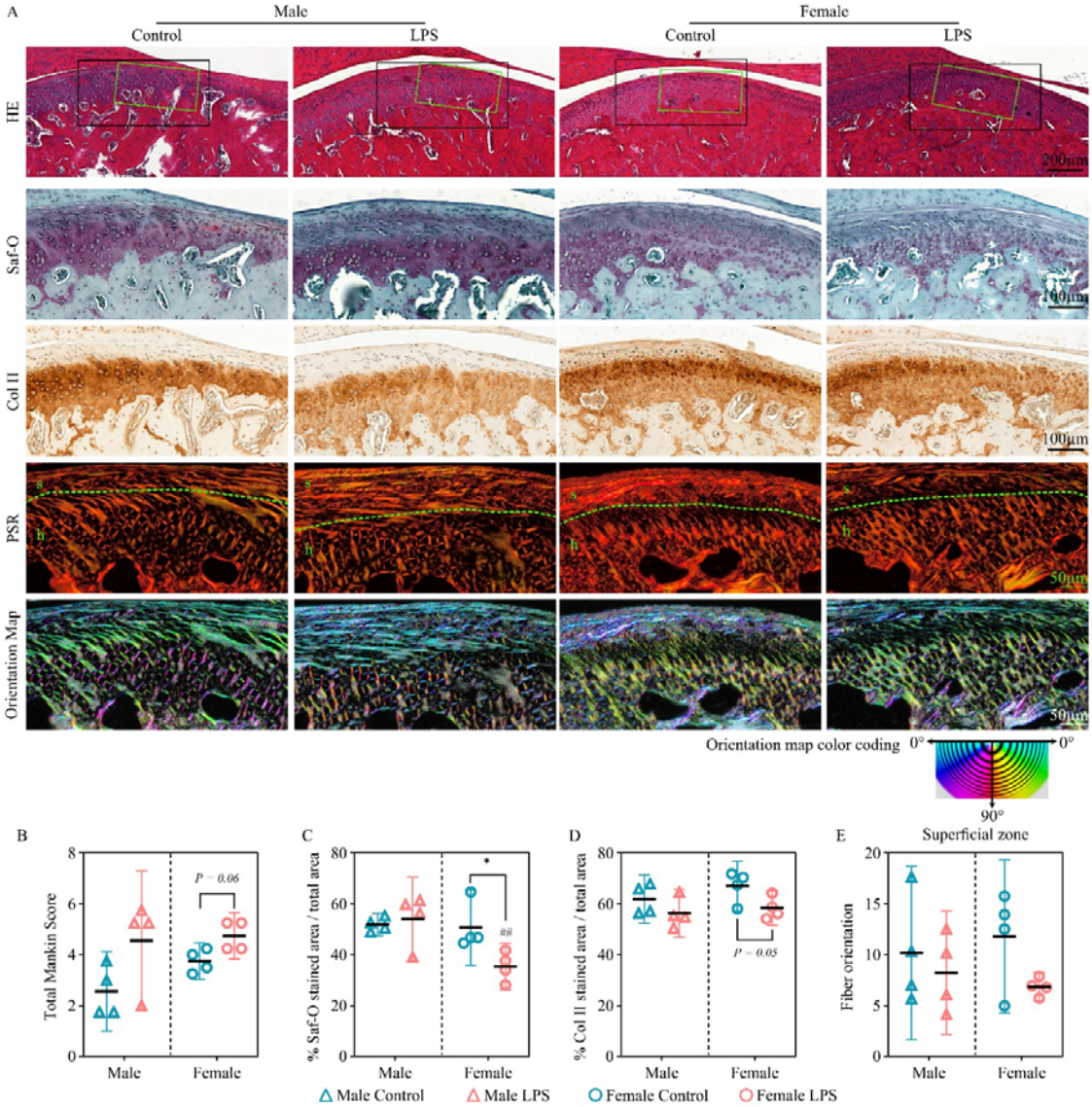

Figure 2. Histopathological evaluation of TMJ cartilage matrix deposition and ECM fibre organisation in TMJ. (A) Representative images of TMJ stained with hematoxylin and eosin

(HE), safranin-O and fast green (Saf-O), collagen II (Col II), picrosirius red (PSR) imaged using a polarized microscope, and pseudo-colour orientation maps of PSR to visualise the fibre orientation (s: superficial zone; h: hypertrophic zone). The black boxes in the HE image indicate the regions where high magnification Saf-O and Col II images were taken, whereas the green boxes indicate the region where high magnification PSR images were taken. Scale bar: 200µm (HE), 100 µm (Saf-O and Col II), 50 µm (PSR and orientation map). (B) Total Mankin score for the cartilage degeneration. Quantification of (C) safranin-O-stained area (Saf-O^+) and (D) collagen II-stained area (Col II^+) in condylar cartilage. (E) Fibre orientation of the superficial zone. Data represent the mean with 95% CI. * $P < 0.05$ compared to the control group within the same sex. N = 4 animals per group and sex.

Changes in bone structural parameters were quantified by µCT (Figure 3A). Biological sex has a dominant effect on the trabecular architecture. Compared with males, females had significantly lower total bone volume fraction and thinner trabecular bones. (Figure 3B). LPS exposure further reduced trabecular number by 2% and increased trabecular separation by 11% in females compared to controls (Figure 3B). This structural deterioration was not seen in male rats. The BMD was not affected by LPS in both sexes. Based on HE staining and Krenn's score, mild synovitis was observed only in the female LPS group, with a mean difference of 0.75 (95% CI: 0.27–1.23; $P = 0.029$) compared with the female control (Figure 3C, D). No significant difference was noted in any of the subcategories in either sex (Supplementary Figure 4).

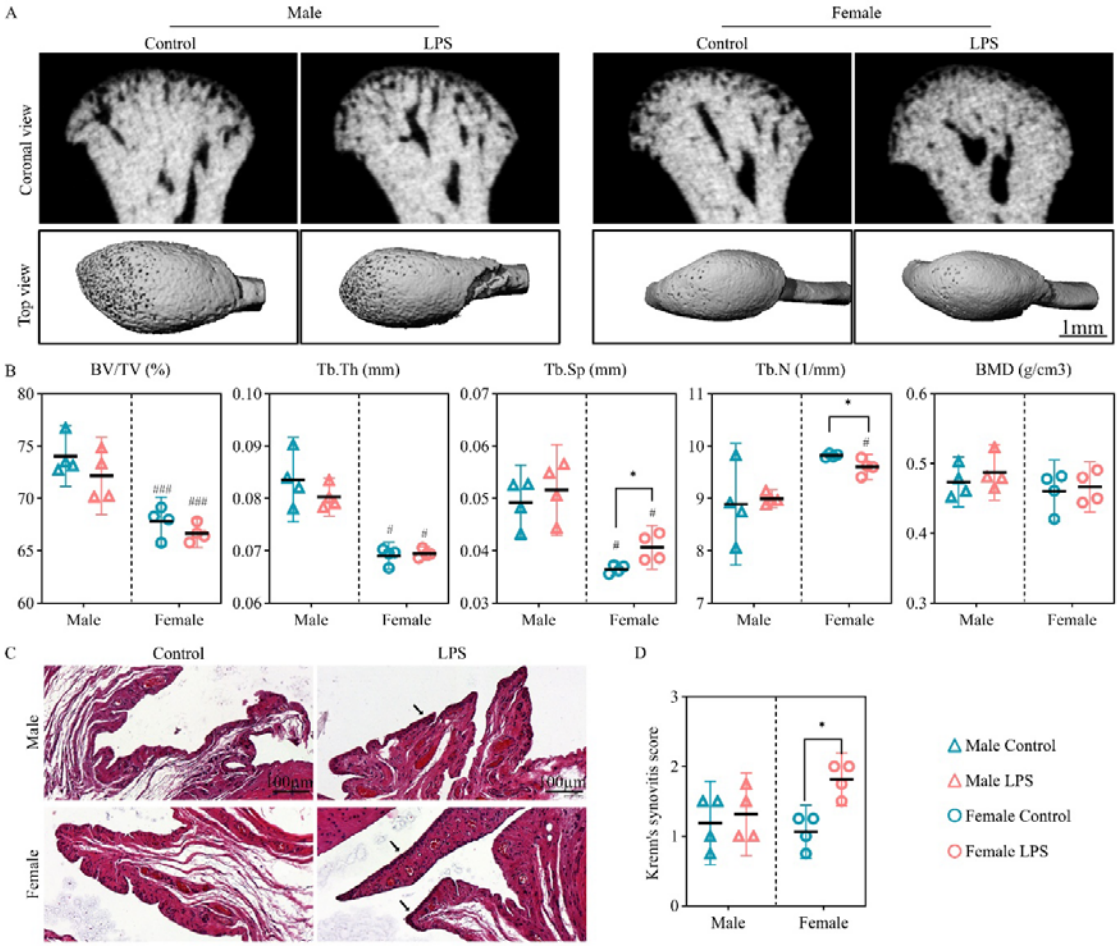

Figure 3. Assessment of subchondral bone structure and synovial membrane inflammation in TMJ. (A) Representative µCT images of TMJ condyles in coronal and top views. Scale bar: 1 mm. (B) Quantitative analysis of bone parameters. (C) Histological analysis of TMJ synovial membrane using HE staining; Black arrow indicates the increase of the synovial lining layer. Scale bar: 100 µm. (D) Krenn's synovitis score used to assess overall synovial inflammation. N = 4 rats per group and sex. Data represent mean with 95% CI. * $P < 0.05$ compared to control group within same sex. $^{\#}$ $P < 0.05$, $^{\#\#\#}$ $P < 0.001$ compared to the males within the same treatment group.

3.2. Sex-differentiated expression of leptin, OB-R and iNOS in TMJ cartilage

IHC staining was performed to detect iNOS, a marker for oxidative stress known to play a key role in the pathogenesis of OA [38]. The iNOS^{+} chondrocytes were mainly located at the hypertrophic zones of the central and posterior regions of the TMJ condylar cartilage. The percentage of iNOS^{+} was significantly higher in females than in males (Figure 4A, Supplementary figures 6-8). LPS infusion further elevated iNOS^{+} cells in female cartilage by 10% (Supplementary Figure 8A). Of note, we did not detect LPS in cartilage by IF staining (data not shown), suggesting that other downstream mediators were involved in the sex-differentiated progression of TMJ OA.

To identify downstream mediators, we performed IF staining to characterise the phenotype of chondrocytes expressing iNOS. We observed an intriguing shift in leptin signalling and uncovered its association with iNOS in TMJ cartilage (Figure 4B, Supplementary figures 5–6B). We found more leptin- and leptin receptor (OB-R)- expressing cells in healthy control females than in males. LPS infusion increased OB-R^{+} cells in both sexes, with a greater increase in males than in females (Figure 4B). In contrast, the percentage of leptin^{+} chondrocytes in female LPS groups elevated by 23.6% (95%CI: 2.74 – 44.6%) compared to female controls ($P = 0.03$), which was also 18.3% (95%CI: -2.65 – 39.2%) higher than that in the male LPS group ($P = 0.08$) (Figure 4E). Further colocalization analysis revealed that in the female LPS group, 60.42% (95%CI: 49.61 – 71.24%) cells in the HPF were stained triple positive for iNOS, OB-R and leptin, which was double of that in female control (29.97%, 95%CI: 23.53 – 36.40%, $P = 0.003$) and 26.3% (95%CI: 8.83 – 43.80%) higher than that in the male LPS group ($P = 0.007$) (Figure 4F).

RT-qPCR of the TMJ condylar head revealed that both biological sex and systemic LPS infusion influenced the gene expression profiles of cartilage and bone. Consistent with immunofluorescence findings showing an increased percentage of triple^{+} cells in LPS-treated females, the expression of genes associated with leptin receptor (*OB-R*) and its downstream signalling (*JAK2* and *STAT3*) was significantly upregulated in LPS-treated females compared to same sex controls. In parallel with changes in leptin signalling, genes related to cartilage matrix remodelling (*MMP13*) and fibrosis (*Col6a1* and *Col6a3*) were also upregulated, while Col2a1 expression was reduced in the female LPS group (Figure 4H and Supplementary Figure 9). Clustering analysis stratified by sex showed that LPS and control groups formed distinct clusters in females but not in males, indicating that LPS infusion has a greater impact on females (Figure 4G).

Overall, our findings demonstrate that LPS induces more TMJ osteoarthritic changes in females than in males, including bone resorption, synovitis, cartilage ECM loss, and chondrocyte inflammation. These sex differences in OA progression are associated with differential expression of leptin and its receptor, OB-R.

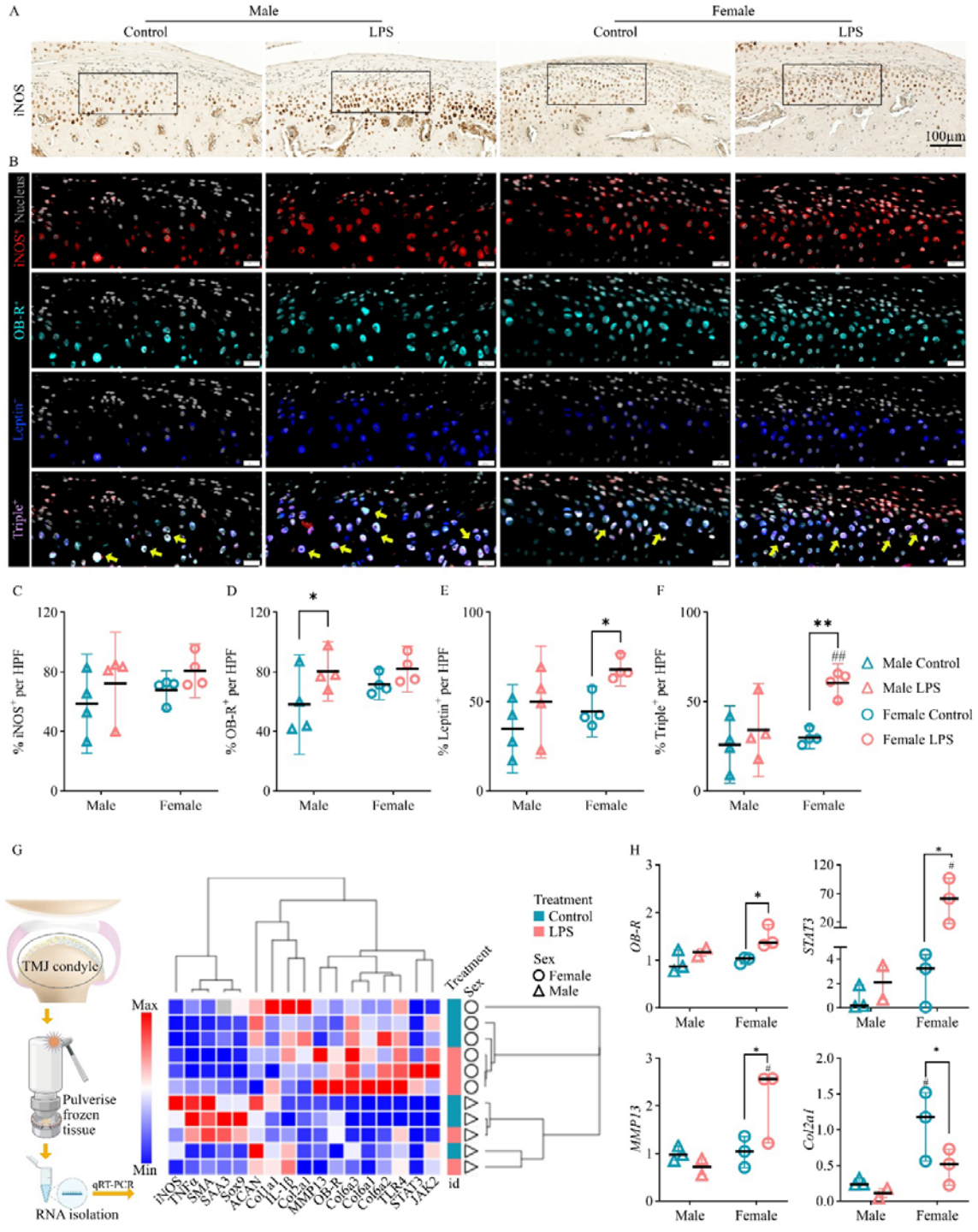

Figure 4. The role of leptin signalling in sex-differentiated OA progression. (A) Representative IHC images showing the expression and distribution of iNOS in cartilage layer. Black box indicating the regions where the high-power field (HPF) of IF images were taken.

Scale: 100µm. (B) Representative IF images showing cell nucleus (grey), iNOS$^+$ (red), OB-R$^+$ (cyan), Leptin$^+$ (blue) and Triple$^+$ (iNOS$^+$OB-R$^+$Leptin$^+$) cells (pink). Scale: 20µm. Quantitative analysis of the percentage of (C) iNOS$^+$, (D) OB-R$^+$, (E) Leptin$^+$ and (F) Triple$^+$ cells over total cells per HPF. N = 4 rats per group and sex. Data represent mean with 95% CI. * $P < 0.05$, ** $P < 0.01$ compared to control group within same sex. $^{\#\#}$ $P < 0.01$ compared to the males within the same treatment group. (G) Heat map depicting gene expression changes of markers associated with LPS, leptin signalling, inflammation, catabolism and cartilage ECM remodelling. The dataset was stratified by sex and clustered according to treatment and genes using one minus Pearson's correlation. (H) selected genes that were most influenced by biological sex and LPS. N = 2–3 rats per sex per group. Data are presented as median with 95% CI. * $P < 0.05$ compared to the control group within the same sex. $^{\#}$ $P < 0.05$ compared to the males within the same treatment group.

3.3 Sex-specific effects of systemic LPS exposure on adiposity and leptin production

After showing the intra-articular localisation of leptin associated with disease status, we next examined its systemic distribution. Blood analysis showed sex-specific positive correlation between leptin and LPS (r = 0.976, n = 8, $P < 0.001$), and NO and LPS ($r = 0.810$, n = 8, $P = 0.015$). More specifically, LPS-treated female rats showed a 3-fold elevation of plasma LPS concentration (0.965 EU/ml, 95%CI: 0.076 – 1.854 EU/ml vs. 0.24 EU/ml, 95%CI: 0.134 – 0.338 EU/ml, $P = 0.029$), accompanied by a 60% increase in plasma leptin (15.74 ng/ml, 95%CI: 11.26 – 20.22 ng/ml vs. 9.86 ng/ml, 95%CI: 6.17 – 13.56 ng/ml, $P = 0.05$) and an 80% increase in NO (45.83 µM, 95%CI: 36.78 – 54.89 µM vs. 25.00 µM, 95%CI: 13.96 – 36.04 µM, $P = 0.06$), compared to female controls. In contrast, males showed no significant changes in plasma LPS, leptin, or NO (Figure 5A).

As leptin is an adipokine primarily produced by white adipose tissue [39], comprehending which fat depot produces leptin in response to LPS infusion may provide important clues to the prevention and treatment of TMJ OA. We showed that adipocyte size increased significantly in response to LPS, despite comparable body weight across groups (Supplementary Figure 9). Relative to sex-matched controls, the size of adipocytes in SAT was increased by 30% in male LPS group (mean difference: 622 µm^2, 95%CI: 254 – 989 µm^2, $P = 0.003$) and by 24% in female LPS group (mean difference: 393 µm^2, 95%CI: 26.2 – 760 µm^2, $P = 0.04$) (Figure 5B). Notably, the enlargement of adipocyte size in VAT was only observed in LPS females, not in males (Figure 5C). Interestingly, although adipocyte hypertrophy was observed in SAT of both sexes, only female SAT exhibited upregulated expression of genes associated with LPS receptor (*TLR4*), inflammation (*TNFα* and *iNOS*), and leptin production (*Leptin*) in response to LPS infusion. The expression of *OB-R* was downregulated in the SAT of LPS-treated males and upregulated in the VAT of LPS-treated females in relation to the sex- and tissue – matched controls (Figure 5 D).

Our data demonstrated that LPS infusion induced systemic damage affecting adipose tissue, particularly SAT, in female rats, leading to aberrant leptin secretion and its release into the blood circulation.

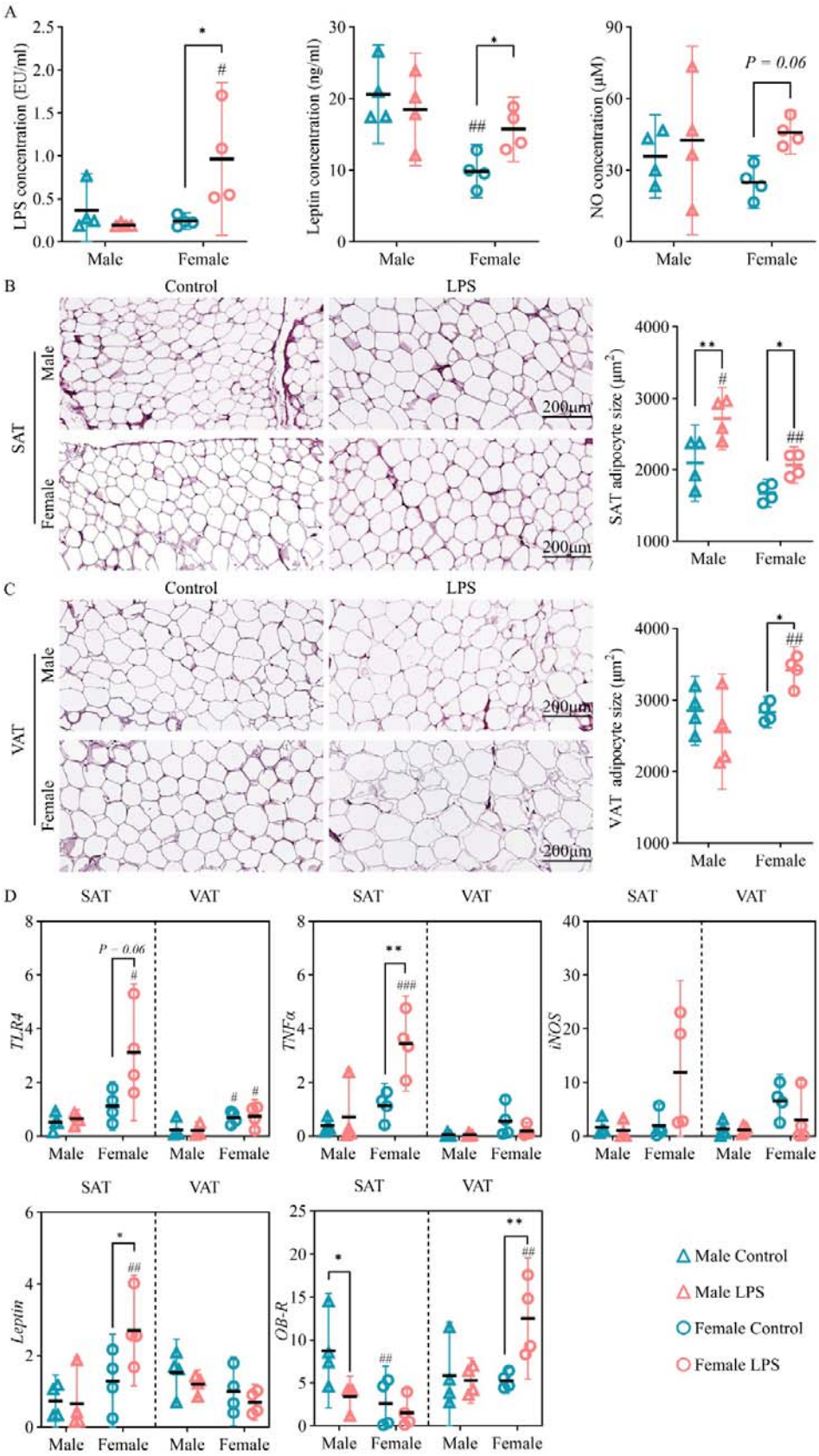
A
LPS concentration (EU/ml)
Leptin concentration (ng/ml)
NO concentration (μM)
P = 0.06
Male
Female
B
Control
LPS
SAT
Male
Female
200μm
SAT adipocyte size (μm²)
C
VAT
VAT adipocyte size (μm²)
D
SAT
VAT
TLR4
TNFα
iNOS
Leptin
OB-R
Male Control
Male LPS
Female Control
Female LPS

271

Figure 5. LPS infusion induces sex-specific changes in adipose tissue and leptin production. (A) The concentration of LPS, leptin and nitric oxide (NO) in the blood plasma. The representative HE staining of adipose tissues and the size of adipocytes in (B) subcutaneous adipose tissue (SAT) and (C) visceral adipose tissue (VAT). Scale bar: 200µm. (D) Gene expression changes in SAT and VAT. Data are represented mean with 95% CI. N = 4 animals per group. * $P < 0.05$, ** $P < 0.01$ compared to control group within same sex. $^{\#}$ $P < 0.05$, $^{\#\#}$ $P < 0.01$ and $^{\#\#\#}$ $P < 0.001$ compared to the males within the same treatment group.

3.4 The effect of leptin on chondrocyte metabolism and oxidative stress

Next, we performed *in vitro* experiments to investigate the role of leptin and its potential synergistic effect with LPS in chondrocytes. The biological sex of the cells was confirmed by agarose electrophoresis (Figure 6A) prior to assigning them to each experiment (Figure 6B). Using Nile red staining, we observed lipid droplet (LD) accumulation in untreated chondrocytes of both sexes (Figure 6C). Upon treatment with increasing doses of leptin, the cells lost their intracellular LDs (Figure 6D). The dose-dependent loss of LDs in female chondrocytes was accompanied by the decline of the metabolic rate, with 8% decrease at 2 ng/ml leptin and a 15% reduction at 20 ng/mL leptin. In contrast, the metabolic rate of male chondrocytes was not affected by changes in LDs, remaining above 95% and significantly higher than that of females at all leptin doses (Figure 6E). Furthermore, female chondrocytes were more sensitive to leptin-induced oxidative stress than male cells. NO production in female chondrocytes increased by 250% with 5 ng/ml leptin treatment and by over 300% with 10 ng/ml leptin ($P < 0.05$), whereas in male cells, NO production remained at baseline with 5 ng/mL leptin and increased only with 10 ng/mL or higher (Figure 6F).

A 3D pellet culture system was used to assess the individual and synergistic effects of leptin and LPS (Figure 6B). Treating healthy cells with 20 ng/ml leptin increased *STAT3* expression in females and significantly upregulated *iNOS* expression in both sexes (Figure 6G). LPS pre-conditioning markedly increased oxidative stress and expression of catabolic genes in chondrocytes, independent of sex (Figure 6H). Leptin treatment on LPS-primed cells synergistically increased *IL-6* gene expression in both sexes but only upregulated *MMP13* gene in females. Interestingly, it also reduced LPS-induced *iNOS* gene expression in female chondrocytes (Figure 6I).

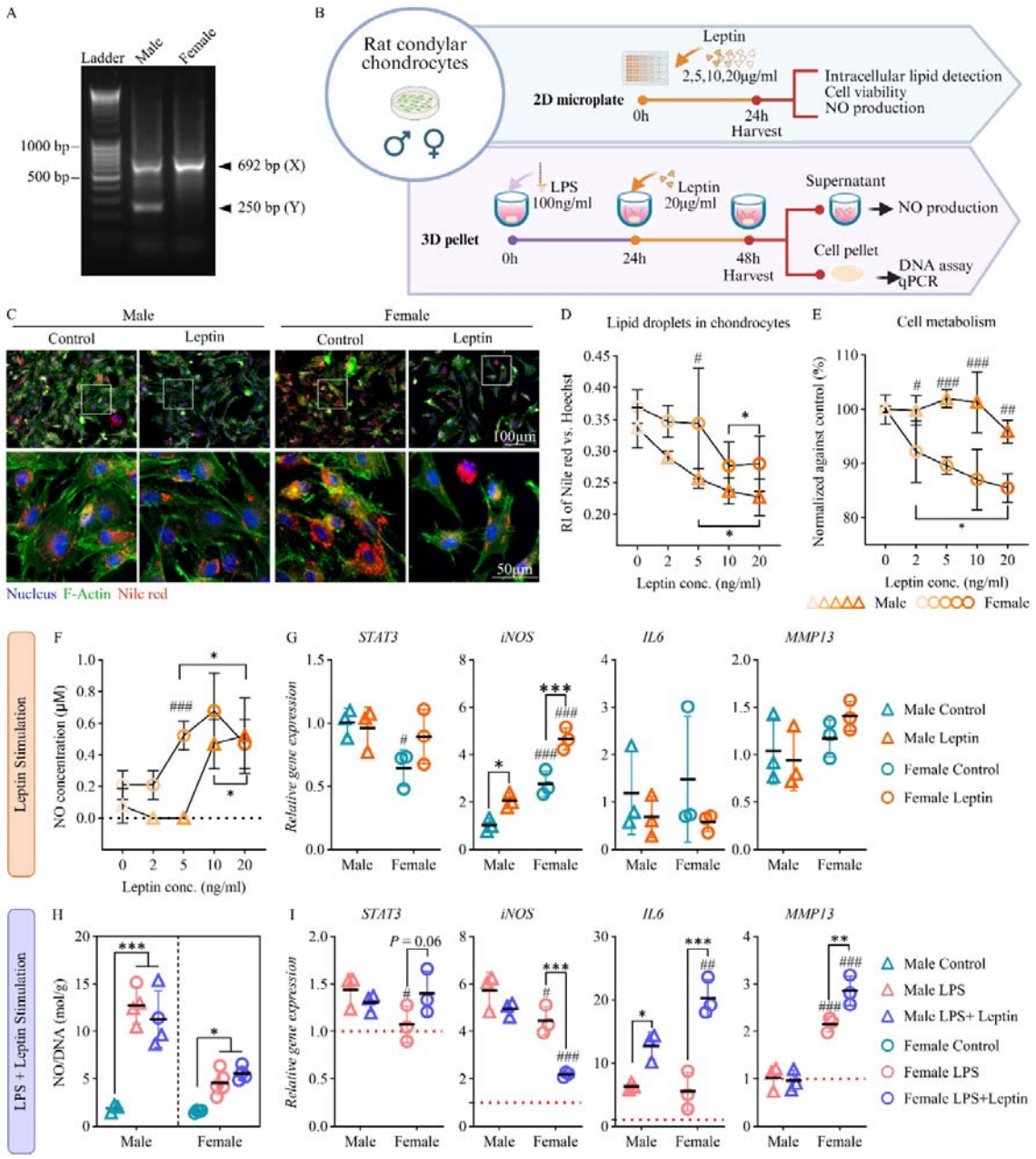

Figure 6. Leptin action in male and female chondrocytes. (A) Agarose electrophoresis to verify the biological sex of the primary rat chondrocytes. (B) Schematic illustration showing the *in vitro* experiment setups. Created in BioRender. Zhang, S. (2026) https://BioRender.com/zbjo4z8. (C) Representative images of Nile red staining showing the changes of lipid droplets in the chondrocytes upon treatment with 20ng/ml of leptin. Lipid droplets were stained with Nile red and shown in red. The cell nucleus was stained with Hoechst and shown as grey. The cell cytoskeleton was stained with F-Actin and shown in green. Top panel: overview of the 2D culture. White boxes indicate where a high magnification image was taken. Scale bar: 100μm. Bottom panel: high magnification images of the chondrocytes. Scale bar: 50μm. N = 3 per group and sex. The dose-dependent changes in (C) intracellular lipid droplet amount, (D) metabolic activity and (F) NO production of

chondrocytes treated with varying concentrations of leptin. (G) gene expression of healthy chondrocyte pellets treated with or without 20ng/ml leptin for 24 hours. (H) NO production normalised against the total DNA and (I) relative gene expression normalised against male controls (red dotted line) of the cell pellets primed with or without100 ng/ml LPS for 24 hours, then treated with or without 20ng/ml leptin for 24 hours. Data represent mean ± SD. N = 3 – 5 per group and sex. * $P < 0.05$, ** $P < 0.01$, *** $P < 0.001$ compared to control group within same sex. $^{\#}$ $P < 0.05$, $^{\#\#}$ $P < 0.01$, $^{\#\#\#}$ $P < 0.001$ compared to males within the same treatment group.

4. Discussion

This study investigated the role of metabolic endotoxemia and its interplay with adipose tissue in the development of MetOA in TMJ. Diet-induced obese rats have been widely used to study the MetOA pathogenesis in knees [40-42] and TMJs [14]. Unlike the knee joint, where animal and human data consistently show that obesity induces OA, studies on the TMJ show a discrepancy between humans and animals. Studies suggested that high BMI might protect the TMJ in humans [11, 12], whereas diet-induced obesity contributed to TMJ OA progression in rats [14]. To address this discrepancy, we postulated that gram-negative bacteria-derived LPS could be a potential mediator driving MetOA, as emerging evidence in the knee shows that LPS occurs alongside obesity in animals on an HFD[18] and induces systemic inflammation[15]. In this study, we infused the animals with LPS for 6 weeks at a dose of 18µg/kg/d, much lower than the doses used in previous studies [15, 25]. Nonetheless, we observed a 3-fold increase in plasma LPS concentration in LPS female rats, similar to the metabolic endotoxemia reported [15], without significant weight change compared to controls. Notably, we did not detect elevations in plasma LPS in males treated with the same dose of LPS. This sex-differentiated development of metabolic endotoxemia was not fully understood, but it may imply that males have a greater capacity to mask or neutralise this chronic low-dose LPS challenge.

We observed that chronic systemic LPS delivery contributed to osteoarthritic changes in the rat TMJ, including loss of GAG and type II collagen, cartilage surface fibrillation, bone deterioration, and synovial inflammation. These effects were significantly greater in female LPS-infused rats than in their male counterparts, consistent with previous observations in the mouse knees [23]. The intra-articular distribution of leptin was also explored. We showed that OA changes in the TMJ were accompanied by sex-specific alterations in the abundance of leptin-dependent NO-producing chondrocytes and by the expression of genes involved in leptin signalling, inflammation, and matrix degradation. These findings are consistent with observations in human knee OA cartilage [43] and in rodents fed with high-fat diets, where adipose-derived leptin mediated or associated with OA severity in the knees [24] and TMJs [14].

Prior studies have shown that leptin is primarily secreted from white adipose tissue in direct proportion to fat content, and it correlates more strongly with adiposity in females due to estrogen [44]. This sex difference was successfully recapitulated in our study. Hypertrophic changes in SAT and VAT adipocytes, accompanied by an increase in circulating leptin concentration, were observed in females in response to LPS, whereas males showed only VAT adipocyte hypertrophy, aligning with human observations [45]. Together, these data suggest that

subcutaneous adipose tissue, particularly in females, may be an important systemic source of leptin-associated signalling in endotoxemia-induced TMJ OA.

Leptin is known to act through with leptin receptors [7] to mediate the downstream NO signalling [46, 47] and GAG synthesis [48] in articular chondrocytes. Our study extends this concept to TMJ chondrocytes and suggests that the response is sex-dependent. Leptin reduced intracellular lipid storage in both sexes, but female chondrocytes appeared more sensitive to this effect. Low leptin doses were sufficient to reduce metabolic activity and increase NO production in female chondrocytes, whereas male cells showed a weaker response. These differences may be explained by sexual dimorphism in cellular energy metabolism, as previous work suggests that female cells rely more on lipid as an energy source, while male cells prefer glucose as a fuel [49]. Consequently, leptin-induced lipid reduction may impose a greater metabolic burden on female chondrocytes.

To further explore whether leptin could amplify inflammatory responses under disease relevant conditions, we examined LPS-primed chondrocytes. In LPS-primed female chondrocytes, leptin synergistically promoted the expression of proinflammatory IL6 and matrix-degrading MMP13, while reducing LPS-induced iNOS expression. Our results revealed the complex sex-dependent role for leptin in healthy and diseased chondrocytes and highlighted the potential involvement of lipid metabolism in this process.

This study has several limitations. Although our data support an association between LPS, leptin signalling and OA pathogenesis, establishing causal relationships will require further *in vivo* studies using leptin-deficient ob/ob mice or leptin receptor-deficient db/db mice. Additionally, a comprehensive understanding of LPS- and leptin-associated lipid metabolism in chondrocytes would benefit from advanced techniques such as lipidomic profiling [50]. Finally, anatomical and biomechanical differences between rat and human TMJs may limit the translational relevance of our findings, and further validation in larger animal models or in humanised in vitro systems will be essential.

5. Conclusion

Our findings show that metabolic endotoxemia induces sex-specific TMJ OA changes in rats, with a greater susceptibility in females, and is associated with a leptin-linked inflammatory response. *In vitro* experiments further supports the sex-differentiated effect of Leptin on healthy and diseased chondrocytes. Overall, our results support a potential female-biased systemic-to-local adipose-cartilage link between metabolic endotoxemia and TMJ OA (Figure 7). This study provides novel insights that may inform future sex-aware and metabolism-targeted therapeutic strategy for TMJ OA.

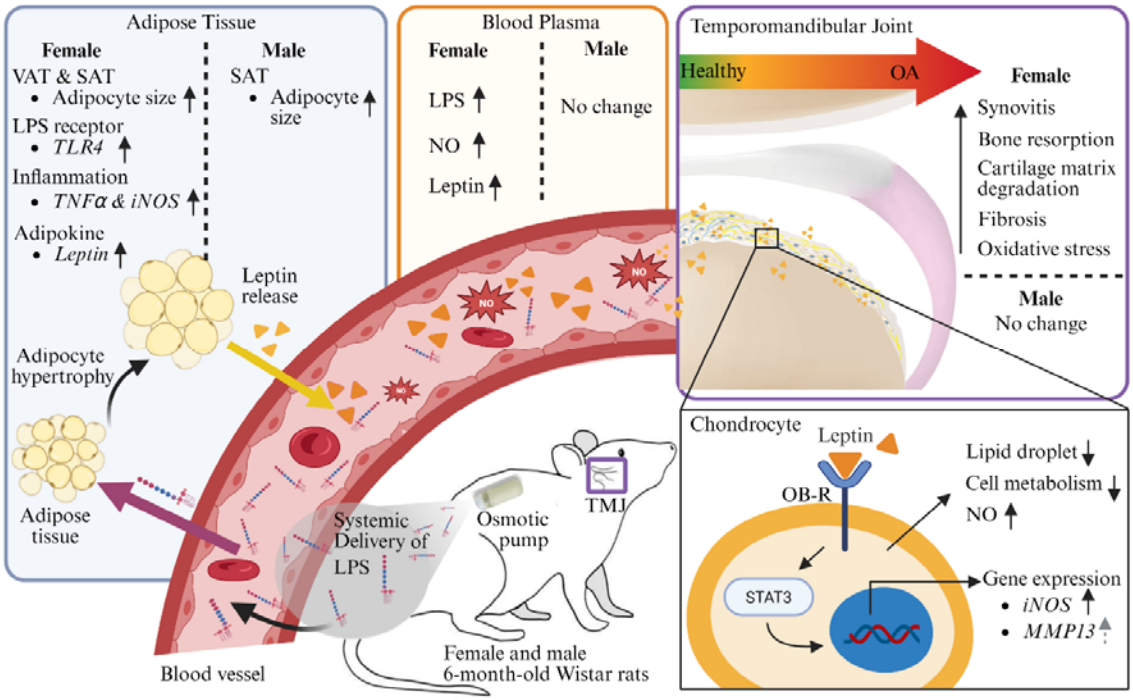

Figure 7. Proposed mechanism of LPS and its interplay with adipose tissue in driving the sex-specific development of TMJ OA. Created in BioRender. Zhang, S. (2026) https://BioRender.com/fttwrav.

Author Contributions

S.Zhang contributed to conception, design, data acquisition, analysis, and interpretation, drafted and critically revised the manuscript; S.Chen contributed to data acquisition, analysis, and critically revised the manuscript; M.Fonti contributed to data acquisition, analysis, and critically revised the manuscript; D.Fercher contributed to design, data acquisition, and critically revised the manuscript. All authors gave final approval and agreed to be accountable for all aspects of the work.

Role of the Funding Source

This project has received funding from the European Union's Horizon Europe Research and Innovation Programme under grant agreement No 101095084. This work was supported by the Swiss State Secretariat for Education, Research and Innovation (SERI) under contract number 22.00462.

Conflict of Interest

The authors declare no potential conflicts of interest with respect to research, authorship, and/or publication of this article.

Declaration of generative AI in scientific writing

During the preparation of this work, the author(s) used ChatGPT 5.2 to correct language.

Data availability

The data that support the findings of this study are openly available in the ETH Zurich Research Collection under the DOI:https://doi.org/10.3929/ethz-c-000797498.

References

1. Boyd RL, Gibbs CH, Mahan PE, Richmond AF, Laskin JL. Temporomandibular joint forces measured at the condyle of Macaca arctoides. American Journal of Orthodontics and Dentofacial Orthopedics 1990; 97: 472-479.
2. Mercuri LG. Temporomandibular Joint Facts and Foibles. J Clin Med 2023; 12.
3. Wang XD, Zhang JN, Gan YH, Zhou YH. Current understanding of pathogenesis and treatment of TMJ osteoarthritis. J Dent Res 2015; 94: 666-673.
4. Alzahrani A, Yadav S, Gandhi V, Lurie AG, Tadinada A. Incidental findings of temporomandibular joint osteoarthritis and its variability based on age and sex. Imaging Sci Dent 2020; 50: 245-253.
5. Yadav S, Yang Y, Dutra EH, Robinson JL, Wadhwa S. Temporomandibular Joint Disorders in Older Adults. J Am Geriatr Soc 2018; 66: 1213-1217.
6. Zapata-Linares N, Loisay L, de Haro D, Berenbaum F, Hügle T, Geurts J, et al. Systemic and joint adipose tissue lipids and their role in osteoarthritis. Biochimie 2024; 227: 130-138.
7. Ait Eldjoudi D, Cordero Barreal A, Gonzalez-Rodríguez M, Ruiz-Fernández C, Farrag Y, Farrag M, et al. Leptin in Osteoarthritis and Rheumatoid Arthritis: Player or Bystander? Int J Mol Sci 2022; 23.
8. Wei G, Lu K, Umar M, Zhu Z, Lu WW, Speakman JR, et al. Risk of metabolic abnormalities in osteoarthritis: a new perspective to understand its pathological mechanisms. Bone Research 2023; 11: 63.
9. Jiang L, Tian W, Wang Y, Rong J, Bao C, Liu Y, et al. Body mass index and susceptibility to knee osteoarthritis: a systematic review and meta-analysis. Joint Bone Spine 2012; 79: 291-297.
10. Reyes C, Leyland KM, Peat G, Cooper C, Arden NK, Prieto-Alhambra D. Association Between Overweight and Obesity and Risk of Clinically Diagnosed Knee, Hip, and Hand Osteoarthritis: A Population-Based Cohort Study. Arthritis Rheumatol 2016; 68: 1869-1875.
11. Minervini G, Franco R, Marrapodi MM, Almeida LE, Ronsivalle V, Cicciù M. Prevalence of temporomandibular disorders (TMD) in obesity patients: A systematic review and meta-analysis. Journal of Oral Rehabilitation 2023; 50: 1544-1553.
12. Rhim E, Han K, Yun K-I. Association between temporomandibular disorders and obesity. Journal of Cranio-Maxillofacial Surgery 2016; 44: 1003-1007.
13. Li B, Jin Y, Zhang B, Lu T, Li J, Zhang J, et al. Adipose tissue-derived extracellular vesicles aggravate temporomandibular joint osteoarthritis associated with obesity. Clinical and Translational Medicine 2024; 14: e70029.
14. Du J, Jiang Q, Mei L, Yang R, Wen J, Lin S, et al. Effect of high fat diet and excessive compressive mechanical force on pathologic changes of temporomandibular joint. Scientific Reports 2020; 10: 17457.
15. Cani PD, Amar J, Iglesias MA, Poggi M, Knauf C, Bastelica D, et al. Metabolic Endotoxemia Initiates Obesity and Insulin Resistance. Diabetes 2007; 56: 1761-1772.
16. Pussinen PJ, Havulinna AS, Lehto M, Sundvall J, Salomaa V. Endotoxemia is associated with an increased risk of incident diabetes. Diabetes Care 2011; 34: 392-397.
17. Trøseid M, Nestvold TK, Rudi K, Thoresen H, Nielsen EW, Lappegård KT. Plasma lipopolysaccharide is closely associated with glycemic control and abdominal obesity: evidence from bariatric surgery. Diabetes Care 2013; 36: 3627-3632.

18. Collins KH, Paul HA, Reimer RA, Seerattan RA, Hart DA, Herzog W. Relationship between inflammation, the gut microbiota, and metabolic osteoarthritis development: studies in a rat model. Osteoarthritis Cartilage 2015; 23: 1989-1998.
19. Amar J, Burcelin R, Ruidavets JB, Cani PD, Fauvel J, Alessi MC, et al. Energy intake is associated with endotoxemia in apparently healthy men12. The American Journal of Clinical Nutrition 2008; 87: 1219-1223.
20. Parantainen J, Barreto G, Koivuniemi R, Kautiainen H, Nordström D, Moilanen E, et al. The biological activity of serum bacterial lipopolysaccharides associates with disease activity and likelihood of achieving remission in patients with rheumatoid arthritis. Arthritis Res Ther 2022; 24: 256.
21. Huang ZY, Stabler T, Pei FX, Kraus VB. Both systemic and local lipopolysaccharide (LPS) burden are associated with knee OA severity and inflammation. Osteoarthritis Cartilage 2016; 24: 1769-1775.
22. Fotis L, Shaikh N, Baszis KW, Samson CM, Lev-Tzion R, French AR, et al. Serologic Evidence of Gut-driven Systemic Inflammation in Juvenile Idiopathic Arthritis. J Rheumatol 2017; 44: 1624-1631.
23. Mendez ME, Sebastian A, Murugesh DK, Hum NR, McCool JL, Hsia AW, et al. LPS‐Induced Inflammation Prior to Injury Exacerbates the Development of Post‐Traumatic Osteoarthritis in Mice. Journal of Bone and Mineral Research 2020; 35: 2229-2241.
24. Collins KH, Lenz KL, Welhaven HD, Ely E, Springer LE, Paradi S, et al. Adipose-derived leptin and complement factor D mediate osteoarthritis severity and pain. Sci Adv 2025; 11: eadt5915.
25. Uchiumi D, Kobayashi M, Tachikawa T, Hasegawa K. Subcutaneous and continuous administration of lipopolysaccharide increases serum levels of triglyceride and monocyte chemoattractant protein-1 in rats. J Periodontal Res 2004; 39: 120-128.
26. Altman DG, Bland JM. How to randomise. Bmj 1999; 319: 703-704.
27. Bagchi DP, MacDougald OA. Identification and Dissection of Diverse Mouse Adipose Depots. Volume 149, 1940-087X 2019.
28. Weber P, Bevc K, Fercher D, Kauppinen S, Zhang S, Asadikorayem M, et al. The collagenase-induced osteoarthritis (CIOA) model: Where mechanical damage meets inflammation. Osteoarthritis and Cartilage Open 2024; 6: 100539.
29. Asadikorayem M, Weber P, Zhang S, Surman F, Fercher D, Fonti M, et al. In-situ-forming zwitterionic hydrogel does not ameliorate osteoarthritis in vivo, despite protective effects ex vivo. Biomaterials Advances 2025; 169: 214151.
30. Puiggalí-Jou A, Hui I, Baldi L, Frischknecht R, Asadikorayem M, Janiak J, et al. Biofabrication of anisotropic articular cartilage based on decellularized extracellular matrix. Biofabrication 2025; 17.
31. Zhang S, Teo KYW, Chuah SJ, Lai RC, Lim SK, Toh WS. MSC exosomes alleviate temporomandibular joint osteoarthritis by attenuating inflammation and restoring matrix homeostasis. Biomaterials 2019; 200: 35-47.
32. Mankin HJ, Dorfman H, Lippiello L, Zarins A. Biochemical and metabolic abnormalities in articular cartilage from osteo-arthritic human hips. II. Correlation of morphology with biochemical and metabolic data. J Bone Joint Surg Am 1971; 53: 523-537.
33. Krenn V, Morawietz L, Burmester GR, Kinne RW, Mueller-Ladner U, Muller B, et al. Synovitis score: discrimination between chronic low-grade and high-grade synovitis. Histopathology 2006; 49: 358-364.

34. Rezakhaniha R, Agianniotis A, Schrauwen JTC, Griffa A, Sage D, Bouten CVC, et al. Experimental investigation of collagen waviness and orientation in the arterial adventitia using confocal laser scanning microscopy. Biomechanics and Modeling in Mechanobiology 2012; 11: 461-473.
35. Dhakal P, Soares MJ. Single-step PCR-based genetic sex determination of rat tissues and cells. Biotechniques 2017; 62: 232-233.
36. Faul F, Erdfelder E, Lang AG, Buchner A. G*Power 3: a flexible statistical power analysis program for the social, behavioral, and biomedical sciences. Behav Res Methods 2007; 39: 175-191.
37. Faul F, Erdfelder E, Buchner A, Lang A-G. Statistical power analyses using G*Power 3.1: Tests for correlation and regression analyses. Behavior Research Methods 2009; 41: 1149-1160.
38. Ahmad N, Ansari MY, Haqqi TM. Role of iNOS in osteoarthritis: Pathological and therapeutic aspects. J Cell Physiol 2020; 235: 6366-6376.
39. Martínez-Sánchez N. There and Back Again: Leptin Actions in White Adipose Tissue. Int J Mol Sci 2020; 21.
40. Collins KH, Reimer RA, Seerattan RA, Leonard TR, Herzog W. Using diet-induced obesity to understand a metabolic subtype of osteoarthritis in rats. Osteoarthritis and Cartilage 2015; 23: 957-965.
41. Collins KH, Hart DA, Reimer RA, Seerattan RA, Herzog W. Response to diet-induced obesity produces time-dependent induction and progression of metabolic osteoarthritis in rat knees. J Orthop Res 2016; 34: 1010-1018.
42. Collins KH, Hart DA, Seerattan RA, Reimer RA, Herzog W. High-fat/high-sucrose diet-induced obesity results in joint-specific development of osteoarthritis-like degeneration in a rat model. Bone Joint Res 2018; 7: 274-281.
43. Simopoulou T, Malizos KN, Iliopoulos D, Stefanou N, Papatheodorou L, Ioannou M, et al. Differential expression of leptin and leptin's receptor isoform (Ob-Rb) mRNA between advanced and minimally affected osteoarthritic cartilage; effect on cartilage metabolism. Osteoarthritis Cartilage 2007; 15: 872-883.
44. Clegg DJ, Brown LM, Woods SC, Benoit SC. Gonadal Hormones Determine Sensitivity to Central Leptin and Insulin. Diabetes 2006; 55: 978-987.
45. Kennedy A, Gettys TW, Watson P, Wallace P, Ganaway E, Pan Q, et al. The Metabolic Significance of Leptin in Humans: Gender-Based Differences in Relationship to Adiposity, Insulin Sensitivity, and Energy Expenditure*. The Journal of Clinical Endocrinology & Metabolism 1997; 82: 1293-1300.
46. Otero M, Reino JJG, Gualillo O. Synergistic induction of nitric oxide synthase type II: In vitro effect of leptin and interferon-γ in human chondrocytes and ATDC5 chondrogenic cells. Arthritis & Rheumatism 2003; 48: 404-409.
47. Otero M, Lago R, Lago F, Reino JJ, Gualillo O. Signalling pathway involved in nitric oxide synthase type II activation in chondrocytes: synergistic effect of leptin with interleukin-1. Arthritis Res Ther 2005; 7: R581-591.
48. Figenschau Y, Knutsen G, Shahazeydi S, Johansen O, Sveinbjörnsson B. Human Articular Chondrocytes Express Functional Leptin Receptors. Biochemical and Biophysical Research Communications 2001; 287: 190-197.
49. Jain L, Jardim CA, Yulo R, Bolam SM, Monk AP, Munro JT, et al. Phenotype and energy metabolism differ between osteoarthritic chondrocytes from male compared to female patients: Implications for sexual dimorphism in osteoarthritis development? Osteoarthritis Cartilage 2024; 32: 1084-1096.

50. Zhou Q, Ghorasaini M, Cornelis FMF, Assi R, de Roover A, Giera M, et al. Lipidomics unravels lipid changes in osteoarthritis articular cartilage. Ann Rheum Dis 2025; 84: 1264-1276.